Computational Modeling of Carbon Corrosion in PEM Fuel Cells

H.-W. Mindt, K. Jain, A. Gidwani, S. Kumar

This document appeared in

Detlef Stolten, Thomas Grube (Eds.):
18th World Hydrogen Energy Conference 2010 - WHEC 2010
Parallel Sessions Book 1: Fuel Cell Basics / Fuel Infrastructures
Proceedings of the WHEC, May 16.-21. 2010, Essen
Schriften des Forschungszentrums Jülich / Energy & Environment, Vol. 78-1
Institute of Energy Research - Fuel Cells (IEF-3)
Forschungszentrum Jülich GmbH, Zentralbibliothek, Verlag, 2010
ISBN: 978-3-89336-651-4

Computational Modeling of Carbon Corrosion in PEM Fuel Cells

Hans-Wilfried Mindt, ESI-GmbH, Germany
Kunal Jain, ESI US R&D Inc., Huntsville, AL 35806, USA
Ashok Gidwani, CFD Research Corporation, Huntsville, AL 35805, USA
Sanjiv Kumar, Unit Cell Engineering, Ballard Power Systems, Burnaby, BC V5J 5J8, Canada

Proton Exchange Membrane (PEM) Fuel Cells continue to be among the most promising alternative energy devices for automotive as well as stationary applications.

Several modes and mechanisms of degradation of PEM fuel cells, primarily the MEA, have been discussed by de Bruijn et al [1]. Figure 1(B) illustrates the various mechanisms for degradation of electrodes. One such degradation mechanism is the corrosion of carbon supports. Carbon, with an equilibrium potential of 0.207 V at 25 °C, is thermodynamically unstable at typical operating conditions of the fuel cell. Fortunately, slow kinetics allow the use of carbon supports in fuel cells. But, at high electrode potential, the corrosion rate becomes significant. The high potential is mainly caused by mal-distribution of H2. Fuel starvation, or mal-distribution of H2, can also happen due to flooding of the anode or during start-stop cycles, as illustrated in Figure 1 (A).

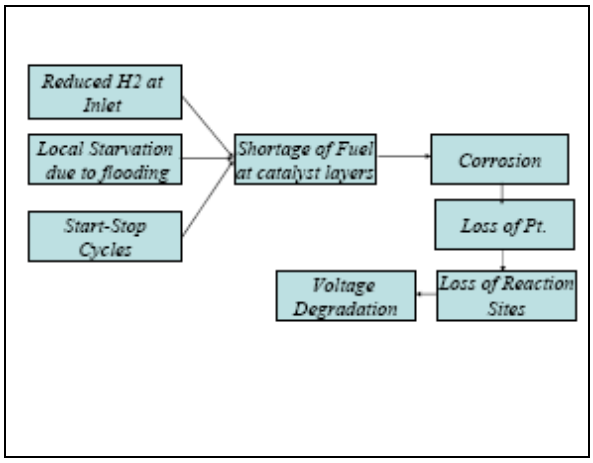

Figure 1 A: Schematic illustrating fuel mal-distribution mode resulting in carbon corrosion.

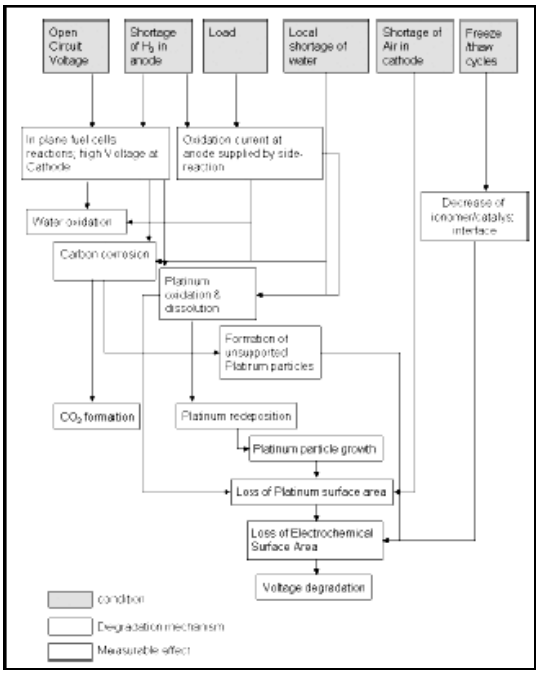

Figure 1 B: Degradation conditions, mechanisms, and effects for electrodes (de Bruijn et al., [1]).

In this work, we numerically study the durability issues of PEM fuel cells due to carbon corrosion in electrodes due to fuel starvation. Understanding of the mechanisms of carbon corrosion and identification of conditions leading to corrosion can help design the operating conditions and guide material development to mitigate the electrode degradation and improve the fuel cell system durability.

The equations governing conservation of mass, momentum, species, and current were solved in a self-consistent manner using a finite volume scheme on arbitrary mesh topology within the framework of the commercial CFD code CFD-ACE+. The details of theory of species transport and electrochemical reactions in porous media, and the mathematical formulation of the conservation equations have been described in detail elsewhere [2,3,9]. Furthermore, species conservations and production/destruction by electrochemical multi-step reactions are considered. Reactants flowing through the pores in a porous solid arrive at the solid catalyst/electrolyte interface by diffusion within the gas pores and the polymer electrolyte. The transfer current is obtained from the Butler-Volmer equation, and has been used in its general form.

1 Model Validation

The developed model was validated against experimental and other model data from the literature. The validation was performed for the cases with and without the carbon corrosion.

1.1 Model Validation for Fuel Cell Operation without Carbon Corrosion

Validation studies were performed against analytical solutions of Newman and Tobias [4] for current through a single porous electrode. Validation was also performed against the experimental data of Ticianelli et al. [5,6]. These studies are reported in detail in our previous publication [2,3] wherein we showed good agreement between the results predicted by our CFD-ACE+ computational model and the analytical/experimental data.

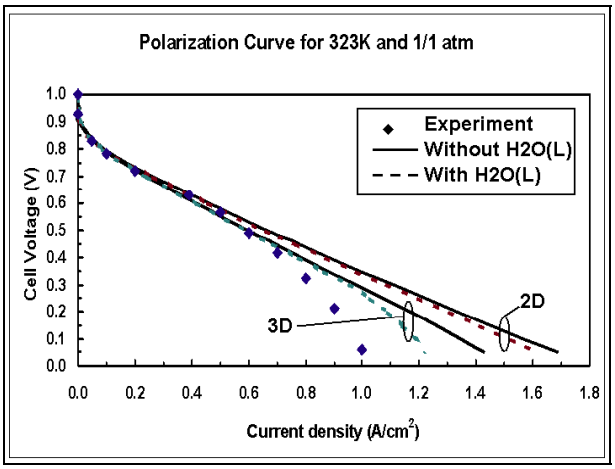

Figure 2: Predicted polarization curve compared against experimental data (Conditions: 323 K, 1 atmosphere pressure and 100 % relative humidity at flow inlet).

Figure 2 presents the polarization curves obtained using two-dimensional and three-dimensional simulations and compares the predicted cell performance with the experimental data. As seen from the polarization curves, at low current densities, there is an excellent match between the computationally predicted data (for both two-dimensional and three-dimensional simulations) and the experimental data. However, as the current density increases, the numerical results overpredict the experimental data, the two dimensional simulation data deviating much more than the three-dimensional simulation prediction. With the inclusion of liquid water formation and transport, the predicted results match better with the experimental data.

1.2 Model Validation for Carbon Corrosion

Carbon corrosion validation studies were performed for air/air polarization for the experimental data reported by UTC-Fuel Cells researchers Meyers and Darling [7]. The channel, GDL, and MEA dimensions and flow rates were same as those in UTC model, and summarized in Table I. The electrochemical reactions and reaction parameters are summarized in Table II. The computational domain with grid is shown in Figure 3. Figure 4 shows polarization curves with air on both electrodes. As explained in Meyers and Darling [7], the current density is negative because current flows through the cell in the direction opposite of normal fuel cell operation. Figure 5 compares the predictions of partial current densities from the current model with the UTC model (Meyers and Darling [7]). The predictions are for air/air case and show excellent match between the two models.

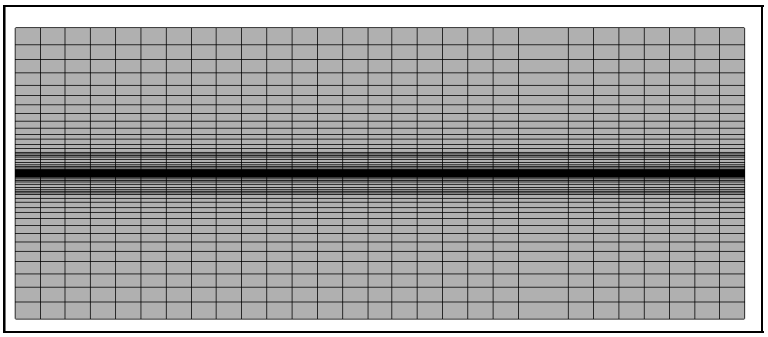

Figure 3: Schematic of the fuel cell with grid distribution. Model scaled in Y by a factor of 100.

Table 1: Channel dimensions and parameters used in this study.

Parameter	*Value*	*Parameter*	*Value*
Length	*711.2 mm*	Fuel Flow Velocity	3.78 m/s
Depth	*0.457 mm*	Air Flow Velocity	10.58 m/s
Width	*1.19 mm*		

Table 2: Electrochemical reactions and parameters used in this study.

Electrochemical Reactions	*Equilibrium Potential*	*Reaction Parameters*	*Value*	*Reaction Parameters*	*Value*
$2H_2 \Rightarrow 4H^+ + 4e^-$	E = 0.0V	$\alpha_{a,H2}$	1	$\alpha_{a,O2}$	0.6
$4H+ + O_2 + 4e^- \Leftrightarrow 2H_2O$	E = 1.2V	$\alpha_{c,H2}$	1	$\alpha_{c,O2}$	1
$C + 2H_2O \Rightarrow CO_2 + 4H^+ + 4e^-$	E = 0.207V			$\alpha_{a,C}$	0.275

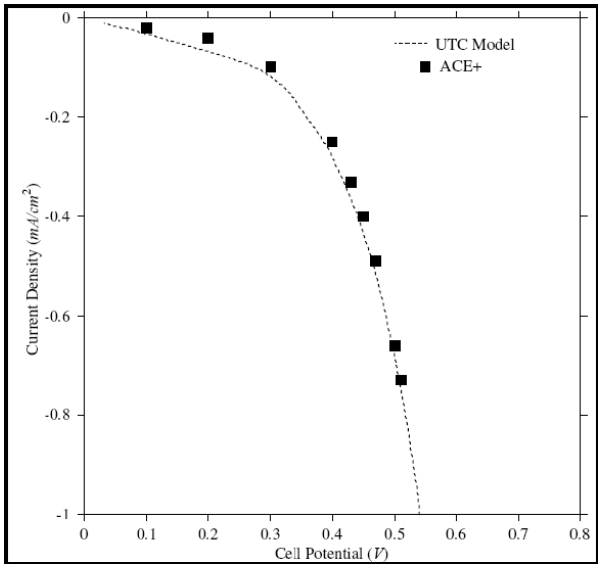

Figure 4: Comparison of air/air polarization data with experimental data reported by Meyers and Darling [7].

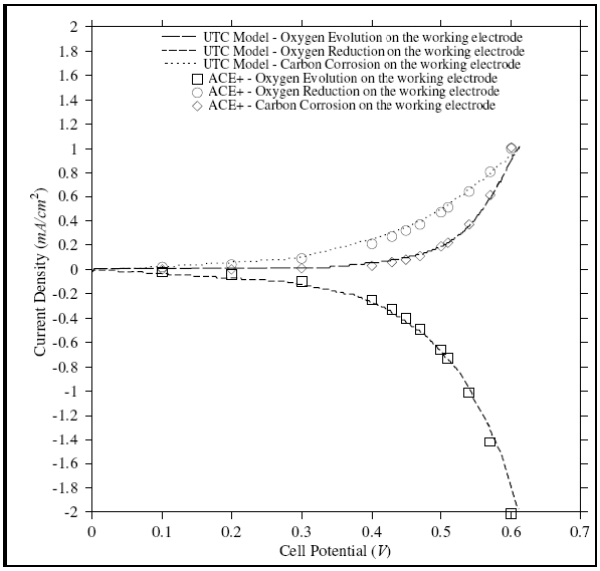

Figure 5: Comparison of partial current densities on the working and counter electrode during air/air polarization curve.

2 Results and Discussion

Having performed model validation, numerical calculations of fuel cell operation under different corrosion conditions were performed in two-dimensional and three-dimensional geometries. The results from these simulations are described in the following subsections.

2.1 Partial starvation due to insufficient hydrogen

This mode of carbon electrode corrosion can occur during start/stop cycles when there is insufficient amount of hydrogen fuel for a brief period of time. We have mimicked this case with a steady state simulation with fuel flow at stoichiometric values less than 1. Figure 6 shows the isocontours of hydrogen mass fraction and corresponding cell potential for three different stoichiometric values for hydrogen. In this case, carbon corrosion reaction is off and the cell is driven with a fixed current density. As seen from the Figure, the fuel concentration decreases as the fuel is consumed downstream. When all the fuel is consumed, the cell potential reverses with electrolysis of water taking place at the working electrode. A transient simulation was performed with carbon corrosion reaction allowed to occur at either electrode.

There was no hydrogen flow in this simulation and air was flown through both channels. A finite number of surface sites for carbon were assumed to be present at the two electrodes. Figure 7 zooms into the catalyst layer and shows the filling of the various carbon sites, C(S), and isocontours of CO2 mass fraction as oxidation of carbon occurs.

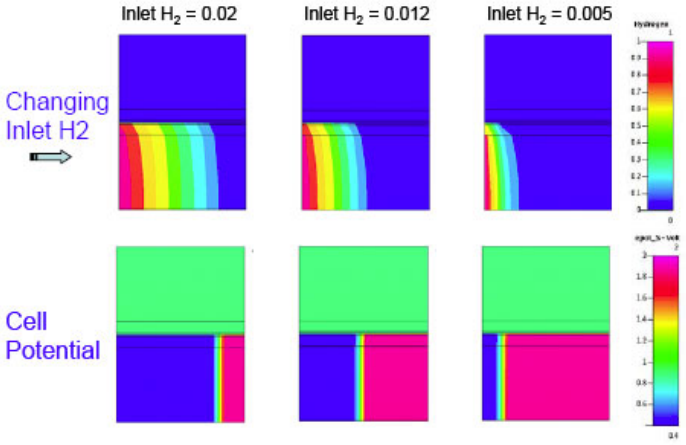

Figure 6: Isocontours of hydrogen mass fraction (normalized) and potential distribution for different stoichiometry values of hydrogen during partial starvation operation; Note: Model scaled in Y by a factor of 100.

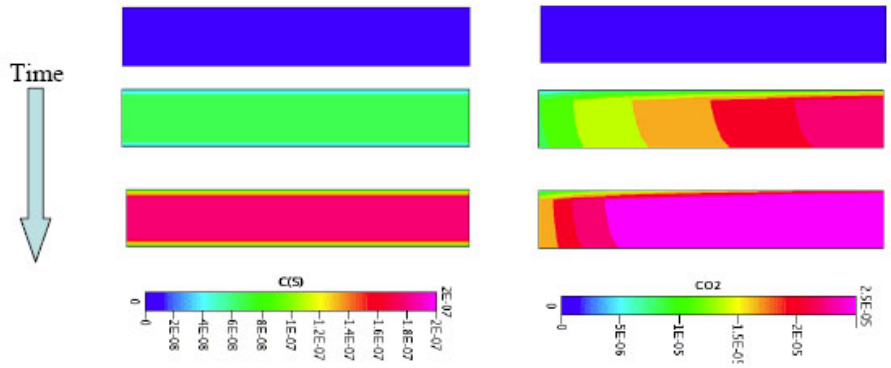

Figure 7: Isocontours of carbon sites (left) and CO2 mass fraction (right) with time illustrating carbon corrosion in the catalyst layer.

2.2 Local starvation

Local starvation of electrode could occur due to localized blocking of catalyst sites by water droplets, which prevents the fuel to reach the active catalyst sites. This situation was mimicked by deactivating the hydrogen oxidation reaction in the blocked region shown in Figure 8. An abrupt decrease in the solid potential is seen where the catalyst site is blocked.

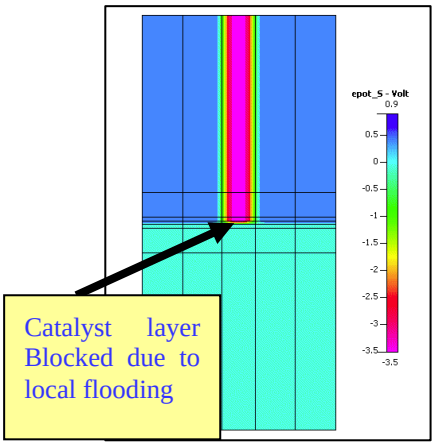

Figure 8: Cell potential distribution during local starvation and carbon corrosion.

2.3 Divided or Dual Cell Reverse-Current Configuration

During start-stop cycles, the fuel electrode may be partially exposed to hydrogen and partially to air. In such a case the region with hydrogen drives the cell while the other half of the cell, which is hydrogen deficient, draws the current and creates the "reversecurrent" conditions. Figure 9(A) depicts the process schematically as it was experimentally demonstrated by Reiser et al. [8] using two electrically connected cells, figure 9(B).

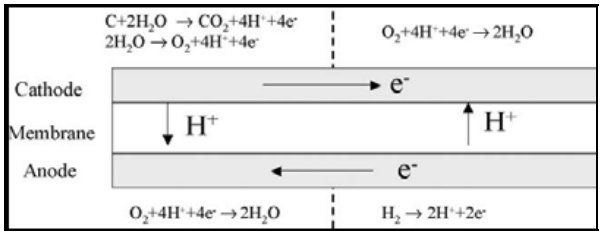

Figure 9 A: Schematic of reverse-current configuration.

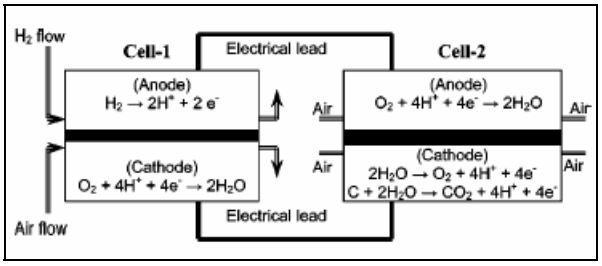

Figure 9 B: Schematic of a dual cell configuration used to simulate the reverse-current condition (Reiser et al.[8])

References

[1] F. A. de Bruijn, V. A. T. Dam, and G. J. M. Janssen, Fuel Cells, 1, 3 (2008).

[2] J. V. Cole and S. Mazumder, J. Electrochem. Soc., 150, A1503 (2003).

[3] J. V. Cole and S. Mazumder, J. Electrochem. Soc., 150, A1510 (2003).

[4] J. S. Newman and C. W. Tobias, J. Electrochem. Soc., 109, 1183 (1962).

[5] E.A. Ticianelli, C. R. Derouin, and S. Srinivasan, J. Electroanal. Chem., 251, (1988).

[6] E.A. Ticianelli, C. R. Derouin, A. Redondo, and S. Srinivasan, J. Electrochem. Soc.,135, 2209 (1988).

[7] J. P. Meyers and R. M. Darling, J. Electrochem. Soc., 153(8), A1432 (2006).

[8] C. A. Reiser, L. Bregoli, T. W. Patterson, J. S. Yi, J. D. Yang, M. L. Perry, and T. D. Jarvi, Electrochemical and Solid-State Letters, 8, A273 (2005).

[9] Ashok Gidwania, Kunal Jainb, Sanjiv Kumarc, and J. Vernon Colea, ECS Transactions, 16(2) 1323-1333 (2008).